Surface Science 143 (1984) 267–286
North-Holland, Amsterdam

ADSORPTION OF OXYGEN ON A Cu{110} SURFACE WITH AND WITHOUT THE INFLUENCE OF A keV Ne^+ BEAM
Stage I: Coverages up to half a monolayer

Th.M. HUPKENS and J.M. FLUIT

Fysisch Laboratorium der Rijksuniversiteit Utrecht, Princetonplein 5, 3584 CC Utrecht, The Netherlands

Received 4 January 1984; accepted for publication 26 March 1984

Low Energy Ion Scattering has been used to study the interaction of molecular oxygen with a Cu{110} surface. The amount of adsorbed atomic oxygen was monitored by the 4 keV Ne^+|O reflection signal. In the first adsorption stage (coverage less than half a monolayer) the sticking probability varied proportional to the number of empty adsorption sites: $S = S_0 (1 - \theta')$. It turned out not to be influenced by the Ne^+ bombardment. The initial sticking probability S_0 was found to be $\simeq 0.24$. In this first adsorption stage the oxygen-covered surface is reconstructed according to the "missing row" model, leading to a (2×1) LEED pattern.

1. Introduction

The dissociative adsorption of oxygen molecules on Cu single crystal surfaces has been the subject of several studies [1–15]. For the O_2/Cu{110} system at room temperature it is known from early LEED observations that two stable structures are formed in successive stages [1]:
- *in stage I:* for small amounts of oxygen, the (2×1) structure (this structure is fully developed at $\simeq 0.01$ Pa s);
- *in stage II:* for exposures up to about 10 Pa s, a c(6×2) structure.

We shall present the results that we obtained for stage II adsorption in a subsequent paper [16].

In an earlier study by our group the oxygen position for stage I was determined by Low Energy Ion Scattering techniques [7,8]: 0.6 Å beneath the first surface layer at the long bridge site. In a subsequent LEIS study [11] it was shown that the (2×1) LEED structure is due to a reconstruction of the Cu{110} surface upon oxygen adsorption: every second [100] row disappears from the surface ("missing row" reconstruction). The existence of this reconstruction has recently been confirmed by a He beam diffraction study [15]. However, in most of the kinetic studies regarding the O_2/Cu{110} system, this reconstruction of the surface was not taken into account.

If one wants to study the kinetics of oxygen adsorption by using Low Energy Ion Scattering, one has to face three major difficulties:
(1) The ion bombardment may damage the surface. In this study damage to the surface was avoided by annealing the surface inbetween the measurements and by using small angles of incidence, if possible. The quality of the surface was checked regularly by measuring the intensity of reflected ions for angles of incidence where all surface atoms should be in each others shadow.
(2) The ion bombardment may influence the kinetics of the oxygen adsorption (apart from the trivial ion-induced desorption). This effect has been reported for the O_2/Cu{110} system under ion bombardment [9]. In the present study the possible influence of the ion beam on the adsorption has been carefully investigated by taking a variety of ion currents.
(3) The signal used to monitor the amount of adsorbed oxygen may not be a simple function of coverage. Coverage dependent neutralization effects as well as coverage dependent shadowing effects may play an important role. In the present study the intensity of Ne^+ ions, scattered from an oxygen atom in a particular direction (the $Ne^+|O$ reflection signal) was taken as a measure for the oxygen coverage. For the angles of incidence used in this study (elevation angle 20°–30°; azimuthal angle not around [100]), it can be shown that this signal is proportional to the coverage up to $\theta = 1/2$ (see section 5). For coverages above half a monolayer (stage II) a much more complicated relation between the signal and the coverage is obtained. This will be discussed in the subsequent paper [16].

In contrast with most other techniques LEIS experiments make it possible – by using shadowing or blocking – to discriminate between oxygen atoms which are adsorbed at essentially different sites. Furthermore, if the $Ne^+|O$ reflection signal is sued a very high surface sensitivity results. Under our experimental circumstances we can be sure that there will be no contribution to the reflection signal from oxygen in deeper layers.

2. Experimental

2.1. Apparatus

The experiments were performed in a stainless steel UHV chamber, pumped by a 500 l/s turbomolecular pump via a LN_2 trap, that also contained a titanium sublimation unit (base pressure $\approx 2 \times 10^{-8}$ Pa). The ion source was differentially pumped by a 200 l/s turbomolecular pump to a pressure of about 2×10^{-6} Pa. The electron-impact source and lens system are described elsewhere [7]; the lens system was modified to make raster scanning of the beam possible. For this purpose the last lens element was replaced by two sets of condenser plates in front of an aperture with diameter of 2 mm. Triangular-

shaped voltages were applied to sweep the ion beam over this aperture. With this provision a beam could be obtained, which was homogeneous within 5% over that part of the target that is seen by the detector [17]. An electrostatic double flat-plate energy analyser, described elsewhere [18] was used. This analyser could be rotated within an accuracy of 2° around the surface in the plane defined by the incoming beam direction and the surface normal. The angular resolution of the analyser was 4°; the energy resolution was 4%. The crystals were mounted in a target manipulator, which has been described elsewhere [19]. With this manipulator the elevation angle of incidence (ψ) could be varied between 0° and 350° (accuracy 0.1°). The sample could be rotated around the surface normal ("azimuthal angle" ϕ) over 370° (accuracy 0.2°). Both rotations were computer-controlled. The sample could be heated by placing an infrared heater in front of the crystal. The temperature was measured at the back of the crystal by a platinum resistance thermometer.

Special care was taken in designing the oxygen inlet system. The oxygen pressure is determined by the flow of oxygen from a small chamber through a needle valve and the pumping speed in the vacuum chamber. The oxygen can be let in or pumped out very rapidly by opening a magnetic valve to a large supply vessel or to a vacuum buffer vessel. If oxygen is let in, the pressure in the main vacuum chamber will reach its final value within 0.5–1 s. If oxygen is pumped out, with this system the oxygen pressure in the chamber will drop to 5% of its initial value within 2 s (see fig. 1), except in cases where high oxygen

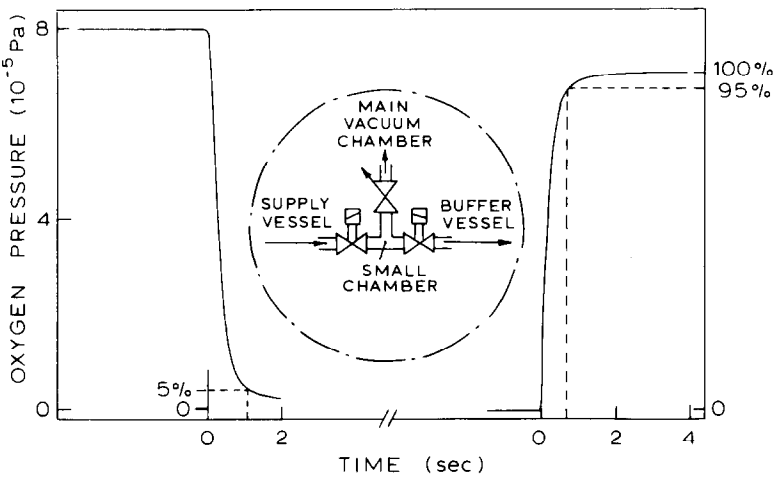

Fig. 1. Oxygen pressure in the main vacuum system after closing the valve to the supply vessel and opening the valve to the buffer vessel and vice versa. The oxygen pressure was measured with a Bayard–Alpert ionization gauge. The partial oxygen pressure monitored with a quadrupole mass analyser produced the same results. A diagram of the oxygen inlet system is shown in the insert. The curves are not corrected for the response time of the recorder ($3\tau = 0.2$ s).

doses were applied (> 0.05 Pa s), because the remaining oxygen pressure will then be determined by the amount of oxygen that is expired by the walls of the apparatus. The great advantage of this system is that the opening of the needle valve can remain practically unchanged if reproducible oxygen pressures are needed. Before and after each measurement the partial oxygen pressure in the exposure room was monitored with a quadrupole mass analyser. The ionization gauge and quadrupole head were located rather far from the target to prevent disturbing effects on the processes under study. Control measurements were performed with the filaments off.

2.2. Preparation of the target

The Cu{110} single crystals were obtained from Material Research Corporation. After the orientation of the 5N single crystal rods had been checked by Laue X-ray back-reflection, disc shaped samples with a diameter of 13 mm and a thickness of 3 mm were spark-cut. The crystals were mechanically and electro-lap polished just before they were mounted in the target manipulator. The surface was further cleaned in vacuum by cycles of annealing (800 K) and ion bombardment (4 keV Ne^+ ions at a small incidence angle) until hardly any contamination could be seen in the energy spectra and until polar distributions showed no surface irregularities (ad-atoms, kinks) except for possible steps present due to a slight misorientation of the crystal surface ($< 0.5°$).

3. Equations for adsorption and ion-induced desorption

We shall express the number of chemisorbed oxygen atoms as the fraction (θ) of the number of copper atoms in the first (unreconstructed) surface layer. The coverage of physisorbed oxygen is very small compared to the coverage of chemisorbed oxygen [20], so it will not give a measurable contribution to the signal used to monitor the coverage of chemisorbed oxygen. The rate of adsorption is determined by the number of oxygen atoms that hit the surface per cm^2 per second ($2i_m$) and by the sticking probability (S), which is the probability that an oxygen molecule that collides with the surface will become dissociatively chemisorbed:

$$\frac{d}{dt} N_s \theta = 2 i_m S(\theta), \tag{1}$$

where N_s is the number of first layer copper atoms per cm^2 (1.09×10^{15}). For oxygen at room temperature i_m amounts to:

$$i_m = 2.7 \times 10^{18} P_{O_2}\ \mathrm{Pa}^{-1}\ \mathrm{cm}^{-2}\ \mathrm{s}^{-1}. \tag{2}$$

When an oxygen-covered surface is bombarded with energetic ions, as is the

case during LEIS experiments, desorption of oxygen will occur:

$$\frac{\mathrm{d}}{\mathrm{d}t} N_s\theta = -i_0\sigma N_s\theta, \tag{3}$$

where i_0 is the ion current density (ions/cm^2 · s), σ is the desorption cross section. The desorption cross section can be interpreted as the depleted surface area (of the initially completely covered surface) per incident ion. The desorption is primarily due to sputtering [21–23]. The desorption cross section may in principle depend on the elevation and azimuthal angles of incidence and on the coverage if the processes leading to desorption are coverage dependent. In the present work care was taken (by chosing the appropriate angles of incidence and detection) that σ did not depend on the coverage.

Thermal desorption of O_{ad} from Cu{110} can be neglected (heat of adsorption 110 kcal/mol O_2). Some apparent desorption may take place due to diffusion (especially if a surface sensitive technique as LEIS is used), but it is generally assumed that oxygen incorporation does not occur at room temperature [1].

If ion-induced desorption is started from a coverage θ_0 and if no oxygen is admitted to the surface, we obtain from eq. (3):

$$\theta(t) = \theta_0 \exp(-i_0\sigma t). \tag{4}$$

During the ion bombardment adsorbed oxygen may be implanted into deeper layers and reappear afterwards. Our measurements and those of De Wit [7] show that this effect is small.

If the surface is bombarded with ions in the presence of oxygen in the gas phase, the adsorption or desorption rate is given by combining eqs. (1) and (3):

$$\frac{\mathrm{d}}{\mathrm{d}t} N_s\theta = 2i_m S(\theta) - i_0\sigma N_s\theta. \tag{5}$$

The Cu{110} surface is saturated in stage I for $\theta_{sat} \simeq 0.5$ [1]. Therefore we define: $\theta' = \theta/\theta_{sat}$. The sticking probability can now be expressed independently of any assumed θ_{sat} by defining $S' = S/\theta_{sat}$. We then obtain:

$$S'(\theta') = \frac{N_s}{2i_m}\left(\frac{\mathrm{d}\theta'}{\mathrm{d}t} + i_0\sigma\theta'\right). \tag{6}$$

If the oxygen exposure is continued, after some time an equilibrium will be reached between the number of adsorbing oxygen atoms and the number of desorbing oxygen atoms. According to eq. (6) the equilibrium coverage θ'_{eq} that is reached ($\mathrm{d}\theta'/\mathrm{d}t = 0$) is given by:

$$\theta'_{eq} = S'(\theta'_{eq})\frac{2i_m}{N_s i_0\sigma}. \tag{7}$$

It appears from all the equations given above that the quantity $i_0\sigma$ rather

than i_0 or σ alone determines the behaviour of all adsorption and desorption curves. Since this quantity can easily be obtained from desorption measurements, it seems a more natural measure for the – direct – influence of the ion beam than i_0 or σ. Therefore in the following sections we shall give all results in terms of $i_0\sigma$. If necessary for comparison with other work, i_0 can be calculated using the desorption cross sections given in ref. [7] or those given in section 5.

4. Measuring methods

Three types of measurements were used to determine the sticking probability function $S(\theta)$.

4.1. "Exposure" method

In this type of measurement the influence of the ion beam is kept as low as possible. The procedure is as follows (fig. 2):
(1) The surface is cleaned by cycles of annealing and ion bombardment.
(2) The ion beam is switched off.

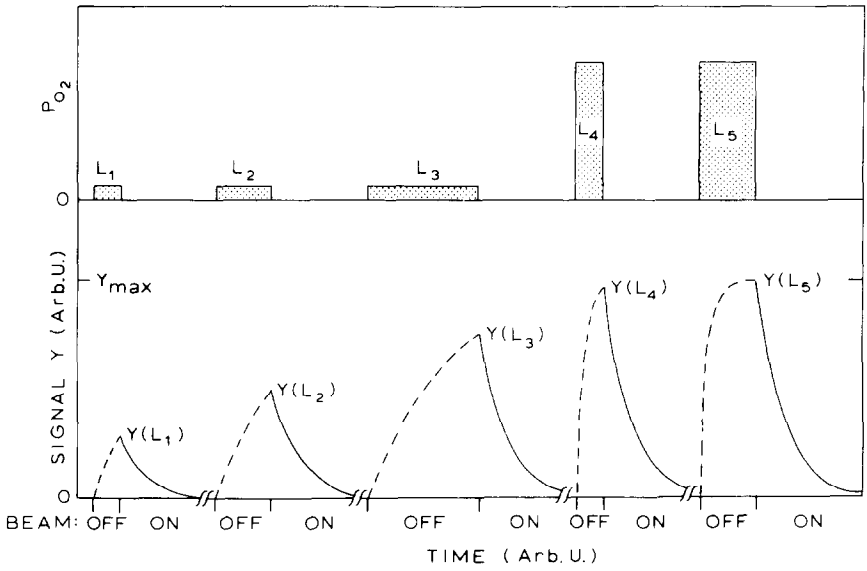

Fig. 2. Illustration of the "exposure" method. The dashed lines indicate the oxygen uptake during the periods that the beam is off. Each shaded area represents the amount of oxygen L_i that is admitted to the surface just before the corresponding signal $Y(L_i)$ is measured.

(3) The surface is exposed to a certain amount of oxygen (L_i).
(4) The oxygen is pumped away (typically 1–3 s).
(5) The signal of Ne^+ ions scattered by the adsorbed oxygen atoms is measured immediately after the ion beam is switched on. This signal is taken as a measure of the oxygen coverage after the corresponding exposure (L_i).
(6) The surface is further cleaned by ion bombardment and the cycle is repeated from point (2), with increasing exposures, at least until the signal of scattered ions reaches a maximum.

When this method is used, it is assumed that the direct influence of the ion beam on the adsorption process is negligible. It was not possible to aneal the surface in between the data points, because it took several hours to cool down the crystal to room temperature, but damage to the surface was prevented by using low angles of incidence during the periods of cleaning.

4.2. *"Time" method*

The influence of the ion beam on the sticking probability function can be studied by simply admitting oxygen at a certain (preset) pressure while the ion beam is on (see fig. 3). The signal of Ne^+ ions reflected from the adsorbed oxygen atoms is taken as a measure of the momentary oxygen coverage. The

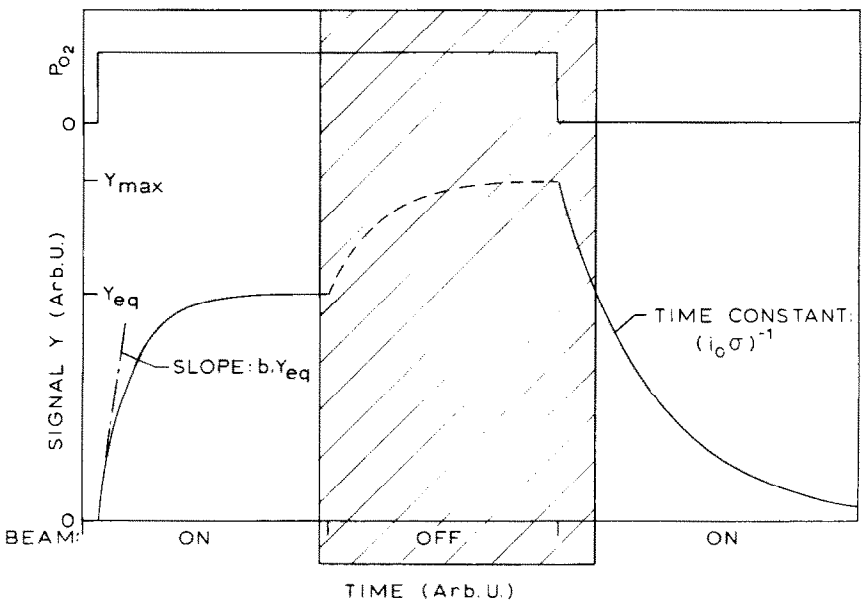

Fig. 3. Illustration of the "time" method. In our case it appeared that the shaded area could be omitted.

maximum coverage in each measurement is obtained when an equilibrium is reached between adsorption and ion-induced desorption. This equilibrium coverage depends on oxygen pressure, ion current density and sticking probability (see eq. (7)). In order to obtain a calibration of the oxygen coverage, it is therefore necessary to measure the saturation coverage with the same ion current density. In principle this can be done by turning off the beam after the equilibrium coverage is reached, during a period of time long enough to obtain the saturation coverage. This, however, is rather difficult in practice for the following reasons:

(a) When the adsorption kinetics are not known beforehand, the amount of oxygen necessary to obtain a saturated surface is essentially unknown. In our case it turned out that when too much oxygen was admitted to the surface the measured signal was less than maximum (this will be shown in a subsequent paper [16]).

(b) The experiments become rather time-consuming, especially if low oxygen pressures are used.

Fortunately, in the course of the experiments it did not appear essential to measure the saturation coverage each time. Therefore, instead of determining the maximum signal (Y_{max}) each time, we measured the relation between the equilibrium signal (Y_{eq}) and Y_{max} in a separate measurement ("pressure" method). Each adsorption measurement could then be followed immediately by a measurement of the desorption rate provided the oxygen could be removed very quickly from the vacuum chamber.

4.3. "Pressure" method

This method involves the measurement of the equilibrium coverage as a function of oxygen pressure. For high oxygen pressures one expects the coverage to be nearly saturated ($\theta_{eq} \simeq \theta_{sat}$). According to formula (7) the equilibrium signal Y_{eq} is given by:

$$Y_{eq} = S'(\theta'_{eq}) \frac{2i_m}{N_s i_0 \sigma} Y_{max}. \tag{8}$$

The maximum signal that is obtained (Y_{max}) is presumed to correspond to θ_{sat}. From this equation it is obvious that the *shape* of the Y_{eq} versus log P_{O_2} curve is only dependent on the $S(\theta)$ relationship. Therefore a horizontal shift of these curves is sufficient to eliminate differences in i_0, σ, S_0, θ_{sat} or N_s. As an illustration the curves for four different $S(\theta)$ relations are shown in fig. 4.

5. Desorption, experimental results

Desorption measurements were performed to obtain information about:

(a) the quality of the ion beam (homogeneity and stability)

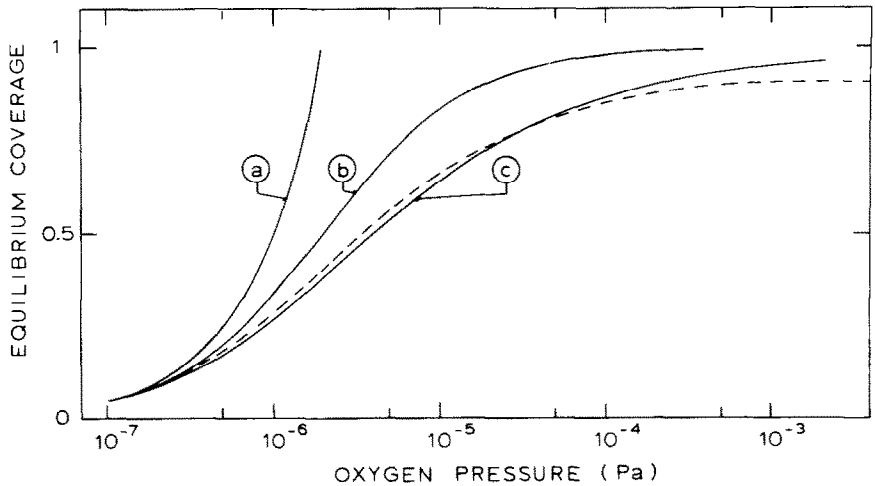

Fig. 4. Theoretical log P_{O_2} versus θ_{eq} curves for some simple $S(\theta)$ relations: (a) $S = S_0$; (b) $S = S_0(1-\theta)$; (c) $S = S_0(1-\theta)^2$. (— — —) Computer simulation for a system in which two adjacent free sites are needed for each oxygen molecule (in four possible orientations). Note that in this case a lower θ_{sat} is reached, because some "single" sites cannot become occupied. The curves were calculated for $S_0 = 1$, $\theta_{sat} = 1$, $N_s = 1.09 \times 10^{15}$ cm^{-2}, $i_0\sigma = 0.01$ s^{-1}. If any of these parameters is changed, the set of curves will be shifted along the horizontal axis.

(b) the relation between the $Ne^+|O$ reflection signal (Y) and the oxygen coverage for several azimuthal angles of incidence (including those directions where shadowing of oxygen ad-atoms by neighbouring atoms is not excluded) (c) the contribution of previously implanted oxygen atoms to the signal

At the same time information was gained about the contribution of several mechanisms to the desorption cross section.

If the trajectory of the Ne^+ ions that scatter from oxygen ad-atoms is sufficiently far from all other surface atoms, we expect the signal to be proportional to the coverage. We then get from eq. (4) for the signal during desorption:

$$Y(t) = Y(0)\exp(-i_0\sigma t). \tag{9}$$

The desorption signal was indeed described very accurately by this equation for $\psi \simeq 20°$ for the azimuthal [011] (see fig. 5) and [211] directions. This is a justification for the assumption that the $Ne^+|O$ reflection signal is proportional to the oxygen coverage. In the [111] azimuthal direction the signal was also described accurately by eq. (9), whereas in this direction one might have expected a large influence of the disappearing reconstruction during desorption (this is discussed in ref. [17], ch. 4).

The small background, which is seen in the measurements, is attributed to multiple scattering of Ne^+ ions in the subsurface region. The reappearance of

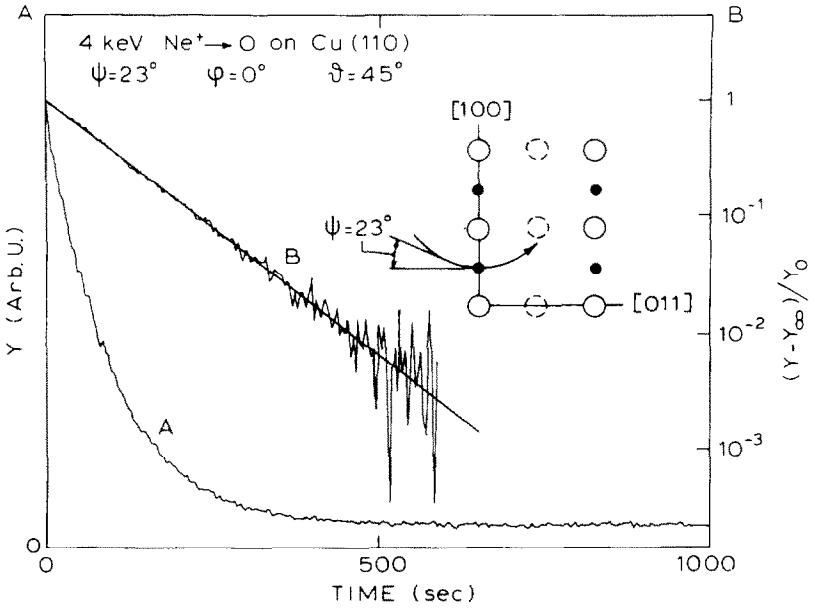

Fig. 5. (A) Typical desorption measurement for any azimuthal direction where the oxygen ad-atoms are clearly "visible" to the beam (in this case the [011] azimuthal direction). (B) The same data points on a logarithmic scale. The beam intensity was $\approx 0.3\ \mu A/cm^2$ ($\approx 2\times10^{12}$ ions/cm^2·s).

previously implanted oxygen atoms could not be detected in any measurement. It should be noted that desorption measurements that were started from coverages above half a monolayer showed considerable deviations from eq. (9). This will be discussed in a following paper [16].

The influence of the beam (in)homogeneity was studied by deliberately making the ion beam inhomogeneous. It appeared that small but significant deviations from eq. (9) occurred even when the ion current density varied by only 5–10% over that part of the target area that is seen by the detector. These deviations showed up for $\theta' < 0.05$.

In the range of azimuthal directions where the oxygen atoms are not directly visible to the ion beam (i.e., $60° < \phi < 90°$) the desorption cross section is not lower than for the directions where the oxygen adatoms are visible. This is in accordance with the results of Taglauer et al. [23] who concluded that sputtering is the main cause of desorption (in the case of keV Ne^+ on O/Ni{110}). This conclusion is sustained by the relatively low cross sections we found for $\phi = 20°$, $\psi = 55°$ ([211]) where the projectiles can penetrate deeply into the channels of the crystal, leading to a relatively low sputtering rate (see table 1).

The result of a desorption measurement for the azimuthal [100] direction, where the oxygen atoms are shadowed and blocked by neighbouring copper

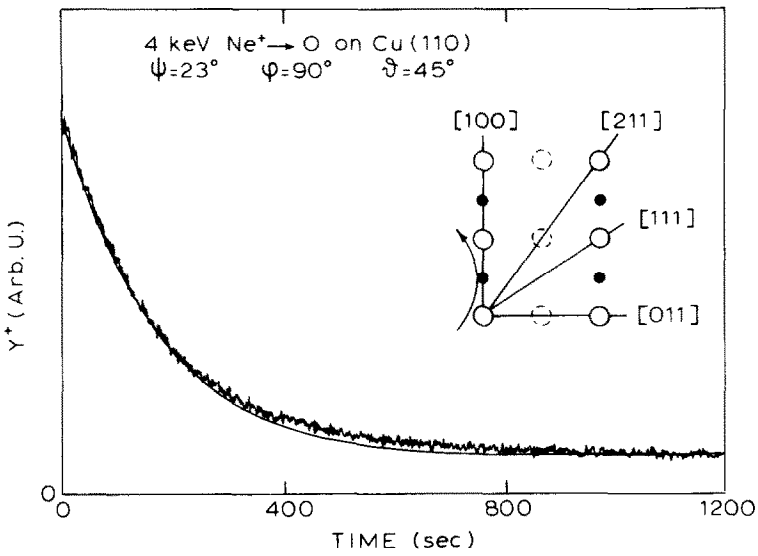

Fig. 6. Desorption measurement, using the positive oxygen recoil signal (Y^+) with a possible contribution of Ne^+|O reflection, for the [100] azimuthal direction, where the oxygen atoms are not directly "visible" to the ion beam (see insert). The beam intensity was ≈ 0.1 $\mu A/cm^2$ ($\approx 8\times10^{11}$ ions/cm^2·s).

atoms is shown in fig. 6. In principle there should be no reflection signal in this situation, but for $\psi = 23°$ it is known from earlier LEIS experiments [11,24] that a broad peak exists in the energy spectra, which is probably due to positive oxygen recoil ions with possibly a contribution of reflected Ne^+ ions. Although the origin of this peak is not clear, we shall assume that it has to do with focussing effects on oxygen atoms at their *normal* positions (evidence for this assumption is given in ref. [17]). The result of a desorption measurement, using the height of this broad peak as a measure for the oxygen coverage, is shown in fig. 6.

The desorption curve shows a typical deviation from an exponential decrease. If it is assumed that the desorption cross section is not coverage-dependent in this case, then it must be concluded that the measured signal is not

Table 1
Desorption cross sections σ for $\psi = 23°$

ϕ	σ (Å^2)
[011]	8
[111]	8
[211]	6–7
[100]	9–16

proportional to the coverage. This seems plausible since multiple reflection will be greatly influenced by small changes in the surface reconstruction and the same is true for neutralization effects. By comparing the times needed to obtain a clean surface it was possible to estimate the desorption cross section for this azimuthal direction (see table 1). The cross section in this direction is larger than it is for other azimuthal directions. This conclusion is confirmed by the measurements described in section 6.3. This is again an indication that sputtering is the main cause of desorption in our experimental situation, and that desorption by direct recoiling is of only minor importance.

6. Adsorption, experimental results

All results given below were obtained for adsorption at room temperature.

6.1. The "exposure" method

The results of an adsorption measurement using the "exposure" method is

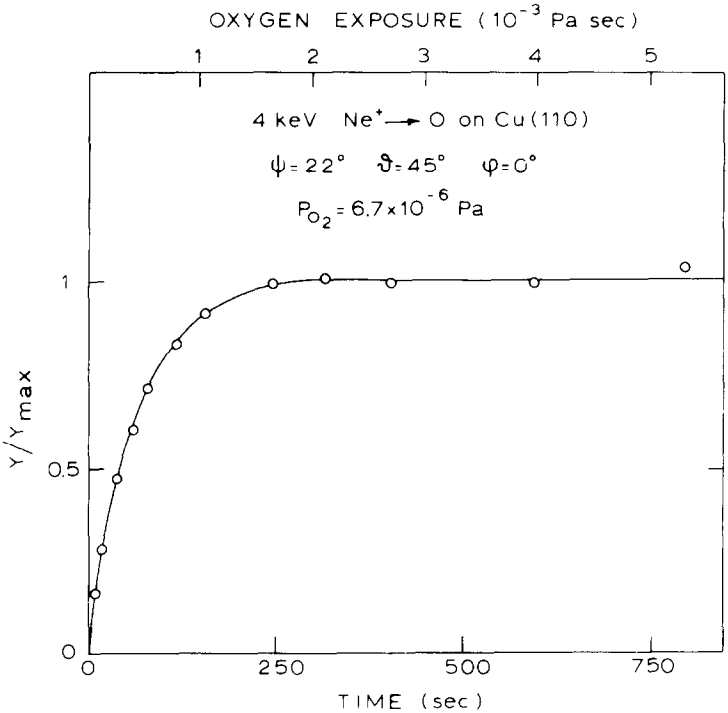

Fig. 7. Adsorption curve, measured with the "exposure" method. The oxygen pressure was kept constant at all exposures so that the exposure scale could be converted into a time scale, to facilitate comparison with other adsorption curves (e.g. fig. 8).

given in fig. 7. The data points can be fitted by a simple equation:

$$\frac{Y}{Y_{\max}} = \theta' = 1 - \exp(-cS_0 Lt), \tag{10}$$

where c is a constant and L the oxygen exposure. The corresponding $S(\theta)$ relation is given by: $S(\theta) = S_0(1 - \theta/\theta_{\text{sat}})$. If it is assumed that the surface is saturated at $\theta_{\text{sat}} = 1/2$, the initial sticking probability is found to be 0.24. This value lies close to values in literature, which were obtained with other techniques (0.17 for ellipsometry combined with AES [10,25] and 0.25 from work function measurements [10,26]).

Note: if errors and error bars are given in the results, they are estimated from the experimental scatter. Systematic deviations from results of other investigators will be mainly due to different pressure readings.

6.2. *The "time" method*

In order to study the influence of the ion beam on the adsorption process, many measurements were performed using the "exposure" method. A typical set of curves is shown in fig. 8. Similar curves were obtained for all oxygen pressures and ion current densities used (pressure range 3×10^{-7}–3×10^{-4} Pa; ion currents up to 9 μA/cm^2, corresponding to a maximum desorption rate $i_0\sigma$ of 0.035 s^{-1}). It turned out that all curves could be fitted satisfactorily by the equation:

$$Y(t) = Y_{\text{eq}}\left[1 - \exp(-bt)\right], \tag{11}$$

where b depends on the ion current density (via $i_0\sigma$) and on the oxygen pressure. From this equation and eq. (6) it can easily be deduced that $S'(\theta')$ is given by:

$$S'(\theta') = \frac{N_S}{2i_{\text{m}}}\left[(i_0\sigma - b)\theta' + b\theta'_{\text{eq}}\right]. \tag{12}$$

In each measurement this relation is measured only up to the equilibrium coverage in that particular measurement. If we assume that eq. (12) holds up to θ_{sat}, we find by putting $S'(\theta'_{\text{sat}}) = 0$ the relation between θ_{eq} and θ_{sat}:

$$\theta'_{\text{eq}} = \frac{Y_{\text{eq}}}{Y_{\max}} = 1 - \frac{i_0\sigma}{b}. \tag{13}$$

Since the experimental scatter in the $Y_{\max}$ values was rather large, probably for the reasons mentioned in section 3.2, eq. (13) could not be checked accurately. Nevertheless it was concluded that large deviations from eq. (13) are not likely to occur. Some evidence for this conclusion was also obtained by a comparison of the absolute yield Y as a function of the primary ion current density i_0, but in general a high accuracy from these comparisons could not be obtained. In

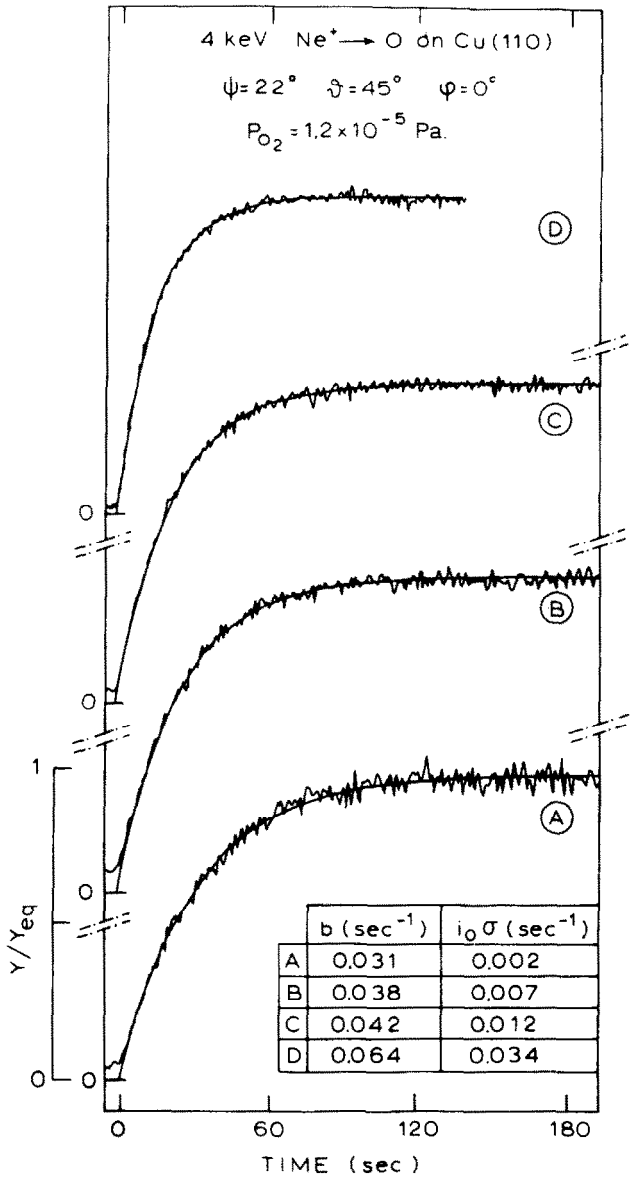

Fig. 8. Set of adsorption curves for increasing primary ion current (1×10^{12} to 2×10^{13} ions/cm^2·s).

view of the above considerations it was decided to leave out the determination of Y_{max}. In this way the total time required for each measurement was considerably reduced. Now, immediately after each adsorption curve had been

measured, a desorption curve was measured under the same experimental conditions, in order to determine the desorption rate $i_0\sigma$ as accurately as possible. From eqs. (14) and (15) it follows:

$$S'(\theta') = \frac{N_s}{2i_m}(b - i_0\sigma)(1 - \theta') = S_0'(1 - \theta'). \tag{14}$$

Thus, the sticking probability with the ion beam on, is proportional to the number of free adsorption sites, just as was the case for the "spontaneous" sticking probability. The initial sticking probability is given by: $S_0 = N_s\theta_{sat}(b - i_0\sigma)/2i_m$. From the experimental results, given in fig. 9 it is clear that the initial sticking coefficient S_0 does *not* depend on the ion beam intensity. Thus, in contrast to earlier reported results [27] ion-induced adsorption is not found (up to primary intensities of 9 μA/cm^2). In that work the sticking probability for $\theta' = 0.6$ increased proportionally to the primary ion intensity. However, those parts of the adsorption curves that corresponded to low coverages were not measured very reliable, due to the high oxygen pressures that were used (usually 1.3×10^{-4} Pa).

Fig. 9 shows only a few results of many measurements. Measurements with a slightly different angle of incidence, with a somewhat different scattering

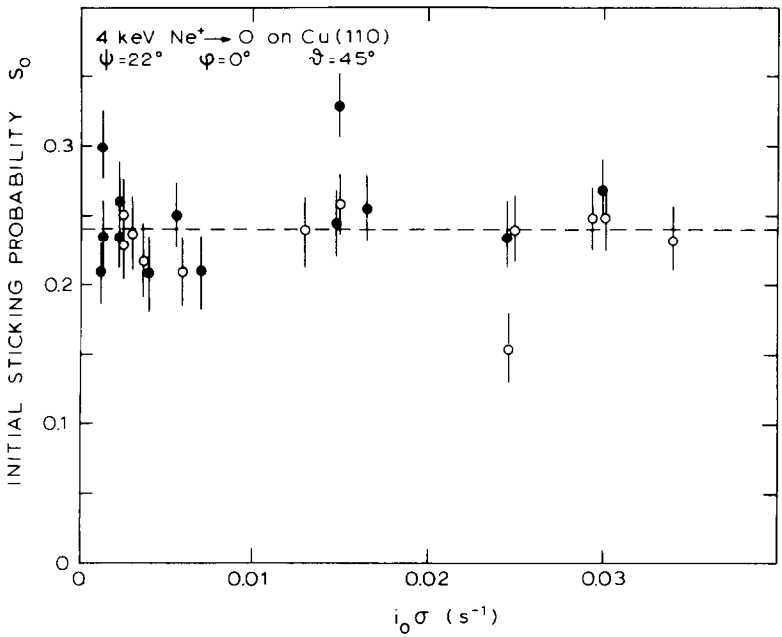

Fig. 9. The initial sticking probability S_0, determined with the "time" method, as a function of the desorption rate $i_0\sigma$.

angle and measurements with two other samples all produced the same results, within experimental accuracy. A few measurements were performed in different azimuthal directions, where the oxygen ad-atoms could also be seen by the ion beam. These measurements too produced the same $S(\theta)$ relation.

Measurements in the [111] azimuthal direction did not deviate from these results, just as was the case for the desorption measurements (see section 5), although a strong influence of the increasing reconstruction of the surface would be expected for this case. This matter is discussed in ref. [17], ch. 4.

6.3. The "pressure" method

A separate experiment was performed to study the behaviour of the equilibrium signal Y_{eq} as a function of oxygen pressure, at a given ion intensity. With $S(\theta') = S_0(1 - \theta')$ we get from eq. (7):

$$\frac{Y_{eq}}{Y_{max}} = \theta'_{eq} = \frac{1}{1 + i_0\sigma/aP_{O_2}S_0}, \tag{15}$$

where a is a proportionality constant. This equation can also be derived from eqs. (13) and (14) by elimination of b.

The result of two measurements is given in fig. 10a. The theoretical curve for $S(\theta) = S_0(1 - \theta')$, with $S_0 = 0.24$, is plotted through the data points. It appears that the fit is very good up to $P_{O_2} \simeq 5 \times 10^{-4}$ Pa. Apparently the $S(\theta)$ relation in stage I does not depend on the way in which a certain coverage is achieved: high pressure and high desorption rate or low pressure and low desorption rate.

Fig. 10b shows equilibrium curves that were measured for some azimuthal angles of incidence. Again the shape of the curves is in agreement with the relation given above. It is particularly interesting to note that the data points for the [100] azimuthal direction could be fitted by the same curve (the curve is shifted to the right due to the larger desorption cross section that is valid for this direction, see section 5). If we assume that the measured signal in this case is related to oxygen atoms at their normal ("stage I") positions, we must conclude from the observations given in section 5 and from the above results that the measured signal in this azimuthal direction is proportional to the oxygen coverage for $\theta' > 0.1$.

It is very interesting to compare our results with those given by De Wit [7] for Ar^+ bombardment (see fig. 11). Much higher desorption rates could be achieved than would be possible with the rastered Ne^+ ion beam of our apparatus. The intensity of sputtered ions ("Secondary Ion Emission" signal: Y_{SIE}) was taken as a measure of the oxygen coverage. Although the type of signal, projectile, intensity and pressure range were different from those used in the measurements given above, the fit of eq. (15) with the data points is

striking. If we used a value for the desorption cross section for 5 keV Ar^+ bombardment, estimated from ref. [7] a value for S_0 was obtained, which was only 20% higher than our result. This difference may be attributed to a different location of the ionization gauges. (Note: A somewhat different definition is used in refs. [7,9]: S_t/θ_{max} and S_n correspond to $2 \times S'$ in the present work.)

The curves of fig. 10 show a tendency for the reflection signal to decrease with increasing oxygen pressure. This effect appears to be real. It is also found for other azimuthal directions of incidence. It would be interesting to know

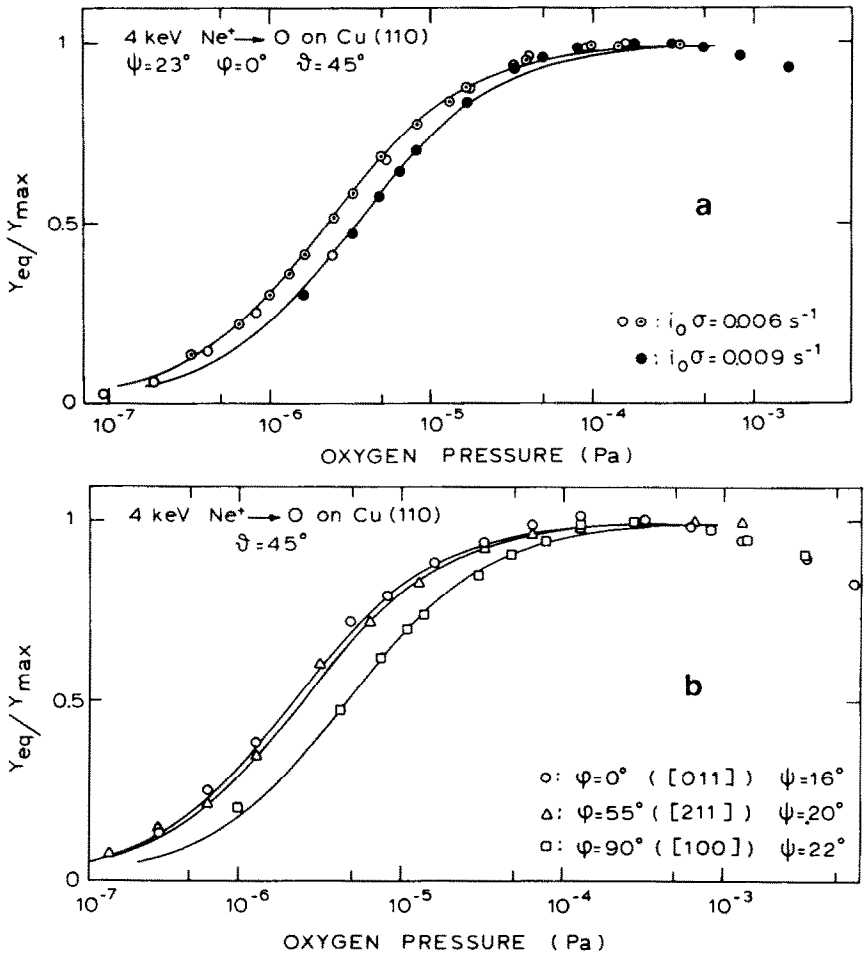

Fig. 10. Equilibrium signal as a function of oxygen pressure. The theoretical curves are plotted through the data points: (a) for two different values of the desorption rate $i_0\sigma$ (beam intensity $\approx 3 \times 10^{12}$ and 5×10^{12} ions/cm^2·s, respectively); (b) for different directions of incidence.

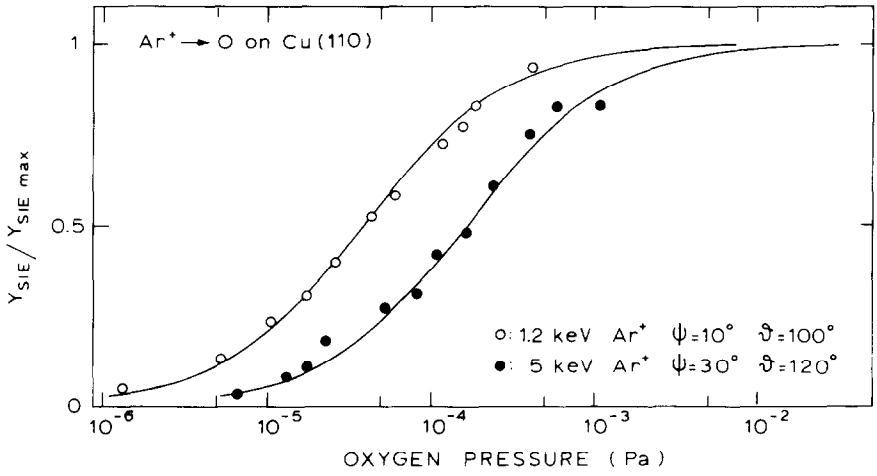

Fig. 11. Equilibrium signal for secondary ion emission as a function of oxygen pressure, measured by De Wit [16]. The theoretical curves for stage I adsorption were plotted through the data points. The curves were shifted horizontally to obtain the best fit.

what would happen in the case of still higher pressures. Our apparatus, however, is not suitable for these higher pressures. It is therefore necessary to study this effect with the "exposure" method. It will be shown in a following paper [16] that this behaviour of the reflection signal can already be attributed to the onset of "stage II" adsorption.

7. Discussion

An important result of the above measurements is that the sticking probability is not influenced by the ion bombardment (within experimental accuracy of about 5%). This is in clear contradiction to results given in an earlier study [27]. One of the main reasons for this discrepancy seems to be that in the earlier study rather high oxygen pressures were applied ($\simeq 10^{-4}$ Pa). With these high pressures the first part of the adsorption curve is necessarily unreliable. Furthermore, Y_{max} may have been determined in the exposure region, where adsorption above half a monolayer takes place (stage II). Since the reflection signal *de*creases in this adsorption stage, this would result in a too low Y_{max} value, and consequently in a too high value for S_0. Another reason for the discrepancy between the two studies may have been that the ion beam was not homogeneous enough for all the ion intensities used in the earlier study. This might also account for the fact that the shapes of some of the adsorption curves are different.

Another important result of the measurements presented in this paper is

that the sticking probability varies in proportion to the number of free adsorption sites. Since oxygen is a diatomic molecule, this $S(\theta)$ relation cannot be explained by simple Langmuir kinetics. In ref. [17] we have given evidence that oxygen adsorbs via a mobile (precursor) state, from which islands of adsorbed oxygen are formed. If large islands are formed this can also account for the fact that the results in the azimuthal [111] direction (adsorption and desorption) did *not* deviate from the results in the [011] and [211] azimuthal directions.

Acknowledgements

This work is part of the research program of the Stichting voor Fundamenteel Onderzoek der Materie (FOM) and was made possible by financial support from the Nederlandse Organisatie voor Zuiver Wetenschappelijk Onderzoek (ZWO).

References

[1] G. Ertl, Surface Sci. 6 (1967) 208.
[2] G.W. Simmons, D.F. Mitchell and K.R. Lawless, Surface Sci. 8 (1967) 130.
[3] T.A. Delchar, Surface Sci. 27 (1971) 11.
[4] A. Oustra, L. Lafourcade and A. Escaut, Surface Sci. 40 (1973) 545.
[5] C. Benndorf, B. Egert, G. Keller, H. Seidel and F. Thieme, J. Vacuum Sci. Technol. 15 (1978) 1806.
[6] P.A. Hofmann, Thesis, Techn. Univ. Munich (1979).
[7] A.G.J. de Wit, Thesis, University of Utrecht (1979).
[8] A.G.J. de Wit, R.P.N. Bronckers and J.M. Fluit, Surface Sci. 82 (1979) 177.
[9] A.G.J. de Wit, R.P.N. Bronckers, Th.M. Hupkens and J.M. Fluit, Surface Sci. 90 (1979) 676.
[10] F.H.P.M. Habraken, Thesis, University of Utrecht (1980).
[11] R.P.N. Bronckers, Thesis, University of Utrecht (1981).
[12] O. Oda, L.J. Hanekamp and G.A. Bootsma, Appl. Surface Sci. 7 (1981) 206.
[13] L.J. Hanekamp, W. Lisowski and G.A. Bootsma, Surface Sci. 118 (1982) 1.
[14] R.H. Milne, Surface Sci. 121 (1982) 347.
[15] J. Lapujoulade, Y. Le Cruër, M. Lefort, Y. Lejay and E. Maurel, Surface Sci. 118 (1982) 103.
[16] Th.M. Hupkens, J.M. Fluit and A. Niehaus, Surface Sci., submitted.
[17] Th.M. Hupkens, Thesis, University of Utrecht (1983).
[18] A. van Veen, Thesis, University of Utrecht (1979).
[19] R.P.N. Bronckers, Th.M. Hupkens, A.G.J. de Wit and W.C.N. Post, Nucl. Instr. Methods 179 (1981) 125.
[20] J.H. de Boer, The Dynamical Character of Adsorption, 2nd ed. (Clarendon, Oxford, 1968).
[21] P. Sigmund, Phys. Rev. 184 (1969) 383.
[22] H.F. Winters and P. Sigmund, J. Appl. Phys. 45 (1974) 4760.
[23] E. Taglauer, G. Marin, W. Heiland and U. Beitat, Surface Sci. 63 (1977) 507.
[24] R.P.N. Bronckers and A.G.J. de Wit, Surface Sci. 112 (1981) 133.

[25] F.H.P.M. Habraken and G.A. Bootsma, Surface Sci. 87 (1979) 333.
[26] F.H.P.M. Habraken, G.A. Bootsma, P. Hofmann, S. Hachicha and A.M. Bradshaw, Surface Sci. 88 (1979) 285.
[27] A.G.J. de Wit, J.M. Fluit, Th.M. Hupkens and R.P.N. Bronckers, Nucl. Instr. Methods 168 (1980) 607; 170 (1980) 471.